IL-17c is involved in olfactory mucosa responses to Poly(I:C) mimicking virus presence

Bertrand Bryche, Aurélie Dewaele, Audrey Saint-Albin Deliot, Claire Le Poupon, Patrice Congar, Nicolas Meunier

IL-17c is involved in olfactory mucosa responses to Poly(I:C) mimicking virus presence

Bertrand Bryche[1], Aurélie Dewaele[1], Audrey Saint-Albin[1], Claire Le Poupon Schlegel[1], Patrice Congar[1], Nicolas Meunier[1,2]

(1) NBO, INRA, Univ Paris-Saclay, 78350 Jouy-en-Josas, France.

(2) Université de Versailles Saint-Quentin en Yvelines, 78000 Versailles, France.

Corresponding author: Dr. Nicolas Meunier nicolas.meunier@inra.fr

Keywords: interleukin-17c, neuromodulation, neurovirology, Poly(I:C), ATP, neuroimmune interaction, olfactory mucosa, olfaction

Abbreviations:

OEC, olfactory ensheathing cells; OM, olfactory mucosa; OSN, olfactory sensory neuron; CNS, central nervous system; IL-17c, interleukin 17c; IL-17c, mouse recombinant interleukin 17c; IL-17ra, interleukin 17 receptor A; IL-17re, interleukin 17 receptor E; Poly(I:C), polyinosinic–polycytidylic; PPADS, pyridoxalphosphate-6-azophenyl-2,4'-disulfonic acid

Abstract

At the interface of the environment and the nervous system, the olfactory mucosa (OM) is a privileged pathway for environmental toxicants and pathogens towards the central nervous system. The OM is known to produce antimicrobial and immunological components but the mechanisms of action of the immune system on the OM remain poorly explored. IL-17c is a potent mediator of respiratory epithelial innate immune responses, whose receptors are highly expressed in the OM of mice. We first characterized the presence of the IL-17c and its receptors in the OM. While IL-17c was weakly expressed in the control condition, it was strongly expressed *in vivo* after intranasal administration of polyinosinic–polycytidylic (Poly I:C), a Toll Like Receptor 3 agonist, mimicking a viral infection. Using calcium imaging and electrophysiological recordings, we found that IL-17c can effectively activate OM cells through the release of ATP. In the longer term, intranasal chronic instillations of IL-17c increased the cellular dynamics of the epithelium and promoted immune cells infiltrations. Finally, IL-17c decreased cell death induced by Poly(I:C) in an OM primary culture. The OM is thus a tissue highly responsive to immune mediators, proving its central role as a barrier against airway pathogens.

Introduction

The olfactory system is composed of a peripheral part: the olfactory mucosa (OM) which represents the sensory organ of detection of odorant molecules within the nasal cavity; and a central part including the olfactory bulb (OB) and other brain structures dedicated to the processing and encoding of olfactory information. Within the OM, olfactory sensory neurons (OSNs) are directly exposed to a variety of potentially harmful environmental agents including viruses, bacteria and environmental chemicals. The axons of the olfactory nerve connect the epithelium of the OM to the central nervous system at the OB *via* the lamina propria and penetrate the skull at the cribriform plate level. Some microorganisms exploit this olfactory pathway and access the olfactory bulb where they can spread to other brain regions like hypothalamus and cortical areas as shown in animal models of infection (Dando et al., 2014; Pägelow et al., 2018). However, infections of the central nervous system by this pathway remain relatively rare in non-immunocompromised subjects, demonstrating the effectiveness of barriers against pathogens within the nasal cavity. The mucocilliary clearance system within the nasal cavity is well described and acts as a very effective innate defence mechanism to eliminate incoming particles and microorganisms from inhaled air (Andersen et al., 1971; Antunes, and Cohen, 2007). The prevention of dissemination of pathogens into deeper tissue also rely on nasal-associated lymphoid tissue (NALT), which can trigger an immune response (Gänger, and Schindowski, 2018). However, very few local defence mechanisms are described and the mechanisms by which immune components act in the OM are not well characterized.

The interleukin-17 (IL-17) family is composed of six members (IL-17a, IL-17b, IL-17c, IL-17d, IL-17e, and IL-17f; (Gu et al., 2013)) that participate in both acute and chronic

inflammatory responses. To date, IL-17c has been identified *in vitro* as an epithelial cell–derived cytokine that enhances mucosal host defence responses in a unique autocrine/paracrine manner (Kusagaya et al., 2013). IL-17c is implicated in the protection against microbial infection and in the pathogenesis of autoimmune disease including multiple sclerosis (Chang et al., 2011) and act as a mediator of respiratory epithelium innate immune response (Pfeifer et al., 2013). Furthermore, a recent study shows that infection of the peripheral nervous system by herpes simplex virus induces the production of IL-17c (Peng et al., 2017). In this study, the authors observed that IL-17c acts as a neurotrophic factor promoting neurite growth of human foetal dorsal root ganglia neurons and provides a survival signal in mouse primary cortical neurons. Transcriptomic studies show a strong expression of IL-17c receptors (IL-17re, IL-17ra) and a potential expression of IL-17c in the OM (Ibarra-Soria et al., 2014; Kanageswaran et al., 2015). Thus, we hypothesized that IL-17c play a role in the immune response of the olfactory epithelium to viral infection and that it may impact the sensory process in the OM by modulating the functioning of OSNs in the mouse.

To explore the role of IL-17c in the OM, we first characterized the presence of the IL-17c system in the nasal cavity of CD1 mice by immunohistochemistry and *in situ* hybridization. While IL-17c was weakly expressed in the control condition, its level was increased under a viral-like context using polyinosinic-polycytidylic (Poly I:C), a Toll Like Receptor 3 (TLR3) agonist. To decipher the impact of IL-17c on olfactory mucosa, we combined electrophysiological, molecular biology and immunohistochemistry approaches using primary culture, and *ex vivo* and *in vivo* experiments.

Materials and methods

Animals and intranasal instillations

CD1 male and female mice (*Mus musculus*) were obtained from multiparous females, and housed in our local animal care facilities (Unité Expérimentale Animalerie Rongeurs (UEAR), Jouy-en-Josas, France) in 12 h light, 12 h dark cycles. Mothers were fed standard chow *ad libitum* and had free access to tap water. All animal experiments were conducted in accordance with the European Council Directive 2010/63/UE and our study was agreed upon by our Local Ethics Committee (APAPHIS#4589). All efforts were made to minimize the number and suffering of mice used. N.M, B.B, P.C holds the Individual Authorization for Performing Experiments in Animals, including the animals experiments conducted in the present study, provided by Préfecture des Yvelines (France), according to French and European laws (agreements #78-154).

Intranasal delivery of Poly(I:C), of mouse recombinant IL-17c (IL-17c : 500ng/mL, 10 µL per nostril) or of vehicle solution were performed in awake mice daily using a specialized intranasal grip adapted from Hanson et al. (2013). Mice received intranasal administration of 20 µg Poly(I:C) sodium salt (P 4287/10 Tocris Bioscience, UK) dissolved in 10 µL of sterile saline into each nostril. The dose of Poly(I:C) used was determined according to a previous study measuring the effect of Poly(I:C) on the OM (Kanaya et al., 2014).

Immunohistochemistry and OM dynamics quantification

The immunohistochemistry from OM tissue sections was performed as described previously (François et al., 2016). The nasal septum and turbinates were removed as a block and post-fixed overnight at 4°C in 4% paraformaldehyde PBS. Blocks were

cryoprotected with sucrose (30%) and cryo-sectioned sagitally (14 µm thickness). Sections were stored at -80°C until use. PCNA staining requires an antigen retrieval in a citrate buffer (pH=6) at 95°C for 30 min. Non-specific staining was blocked by incubation in PBS containing 2% bovine serum albumin and 0.3% Triton X-100. The sections were then incubated overnight with primary antibodies directed against PCNA (1 : 200; mouse monoclonal PC10. GeneTex; Tebu-bio SAS, France) ; cleaved caspase 3 (1: 400; rabbit polyclonal, Cell Signaling; Ozyme, France) ; ionized calcium-binding adapter molecule 1 (1 : 1000; goat polyclonal; Abcam, France) ; or interleukin-17 receptor A (1 : 200; goat polyclonal, R&D systems; Biotechne, France). Fluorescence staining was performed using Alexa-Fluor-488-conjugated goat (1: 1000; Molecular Probes; Invitrogen, France) or Cy^{TM}3-conjugated AffiniPure donkey secondary antibodies (1 : 500; Jackson ImmunoResearch; France). Sections were finally stained with 2 µg/mL Hoechst 33342 for 10 min and mounted in Vectashield after extensive wash in PBS.

Immunohistochemistry was performed on median transversal sections of the OM. For all sections, we took six to eight images situated in caudal, medial or rostral area from the base of the septum to cover the variability of distribution of apoptosis across the OM (Vedin et al., 2009).

Images were taken at x100 magnification using a DMBR Leica microscope equipped with an Olympus DP-50 CCD camera using CellF software (Olympus Soft Imaging Solutions GmbH, OSIS, Münster, Germany), except for cleaved caspase 3 images acquired with an Olympus IX71 inverted microscope equipped with an Orca ER Hamamatsu cooled CCD camera (Hamamatsu Photonics France, Massy, France).

Images were quantified using ImageJ (Rasband, W.S., ImageJ, U. S. National Institutes of Health, Bethesda, Maryland, USA, http://imagej.nih.gov/ij/, 1997–2012)

to threshold specific (François et al., 2016) cleaved caspase 3 and PCNA staining. The same threshold was applied for all images arising from the same experiment. The area of the olfactory epithelium (OE) was measured from the Hoechst staining for cleaved caspase 3 and PCNA signal quantification. Iba1+ cells were counted using the detection particle tool from ImageJ and expressed relative to the OM area as described above.

Hematoxylin and eosin (H&E) staining

After rehydratation, slides were stained in Hematoxylin (H-3404 Vector Laboratories) for 30 s and washed with water. Slides were then transferred in an acid-alcohol solution (0.5% HCl in 70% Ethanol) for 10 s and washed in water, then immersed in Eosin (Sigma HT110316) for 15 s and washed again in water. Finally, slides were gradually dehydrated and mounted in Eukitt (Sigma 25608-33-7). Slides were digitized using NanoZoomer C9600-01 (Hamamatsu).

In situ hybridization

The *in situ* hybridization from OM tissue sections was performed with slight modifications from our previously described protocols (François et al., 2013; Le Bourhis et al., 2014). Briefly, the expression of IL-17c and IL-17re were assessed using digoxigenin (DIG)-labelled RNA probes transcribed *in vitro* (DIG RNA labelling kit from Roche) from target sequences subcloned into a pGEM-T plasmid (Promega) from GenBank (IL-17C nucleotide 242–615, NM_145834.4; IL-17re nucleotide 1152-1626, NM_145826). After rehydration, sections were treated with proteinase K (10 µg/mL) for 10 min at 37°C, washed twice in PBS and incubated in post-fixation solution (4% PFA) for 5 min at 4°C. Sections were then washed in PBS for 10 min at

37°C and incubated in acetylation solution (0.1 M triethanolamine and 0.25% anhydrous acetic acid) for 10 min. The digoxygenin-labeled probes (0.1 µg/µl) were denatured beforehand at 65°C for 5 min then added to the hybridization mix (50% formamide; 2.5% Dextran; 2×SSC; 5x Denhart; 50µg/ml yeast tRNA; 250µg/ml salmon sperm, and 4 mM EDTA) and hybridized overnight at 55°C. Sections were then sequentially washed in 2×SSC (2 ×10 min at 45°C), incubated with RNAse (20µg/mL), washed in 2xSSC (4x5 min at 45°C) and washed in 2xSSC – 30% Formamide (1h at 60°C). Hybridized probes were revealed with NBT-BCIP as substrate in detection buffer and the reaction was stopped by rinsing sections in PBS.

Olfactory mucosa primary cultures

We used a long-term primary culture of mouse OM cells based on a rat OM primary culture described previously (Gouadon et al., 2010). For each experiment, two to three CD1 new-born mice (P4 to P8) were sacrificed by decapitation. The entire OM from turbinates and septum was dissected. After digestion and centrifugation, cells were suspended in sterile Hepes-buffered Dulbecco's Modified Eagle Medium/HamF12 based medium (DMEM/Ham F12; Eurobio, Les Ulis, France) and 10% new-born calf serum (NCS; Eurobio, Les Ulis, France). Cells were counted and seeded at approximately 700 cells/mm^2 on glass coverslips previously coated with poly-L-lysine. Cells were grown at 37°C under 5% CO_2 in the DMEM/HamF12 medium with 10% NCS. Cultures were then treated with one of the following components: Poly(I:C) at 1mg/mL or IL-17c at 200ng/mL.

Assessment of cellular death by lactate dehydrogenase release

The cell death in the primary culture was assessed by quantifying the release of LDH in the culture medium, as previously described (Laziz et al., 2011). Briefly, we measured activities of both the extracellular and the intracellular LDH, respectively from the bathing culture medium and from the primary cultured adherent cells extemporaneously lysed with PBT (PBS 0.5% Triton X-100). The LDH concentration was assayed by the rate of NADH absorbance decrease at 355 nm, using a microplate reader (Tristar LB 941, Berthold technology).

OM slices preparation and calcium imaging

OM slices were prepared from CD1 mouse pups (P5-10) with adaptation from our previous protocol based on rat (Le Bourhis et al., 2014). After the removal of the lower jaw and teeth, the upper skull bone was embedded in 4% low-gelling-temperature type VIIa agarose and placed in ice-cold artificial cerebrospinal fluid (ACSF) solution containing (in mM): 124 NaCl, 5 KCl,1.25 NaH2PO4, 2 MgSO4, 2 CaCl2, 26 NaHCO3 and 10 glucose, saturated with 95% O2 and 5% CO2 at pH 7.4 and ~300 mOsmol/L. Coronal slices (200 µm) were cut using a vibratome (VT1200S; Leica Microsystems, LEICA Microsystemes SAS, Nanterre, France), and kept immersed in oxygenated ACSF at room temperature until use. IL-17c and ATP impact on intracellular Ca^{2+} dynamics in the OM were monitored using the calcium-sensitive dye Oregon green BAPTA-1 (2 mM stock solution in dimethyl sulphoxide), mixed 1 : 1 with 20% Pluronic F-127 (Molecular Probes). After a loading and a washing-out period, slices were transferred into a home-made recording chamber under a 209 long-range water immersion objective (XLUMPLFL20XW, NA 0.95) of an upright microscope (BX51WI, Olympus, Rungis, France), equipped with differential

interference contrast and an infrared video camera. The chamber was continuously gravity perfused with oxygenated ACSF at a rate of 2.5–3 mL/min except when slices were stimulated. Slices were stimulated for 15 seconds with a glass pipette (1MΩ) filled with 10^{-4}M ATP or 500 ng/mL IL-17c under pressure. The pipette was placed at a distance of ~170µm from the apical part of the slice. For off-line analysis of calcium transients, images were background subtracted and changes in fluorescence were calculated relative to the averaged baseline (from 30 s before stimulation) and expressed as $\%\Delta F/F$ (((*F*- $F_{baseline}$)/ $F_{baseline}$)x100) using Xcellence RT software. The general nonspecific purinergic receptor antagonists suramin (100µM) and pyridoxalphosphate-6-azophenyl-2,4'-disulfonic acid (PPADS – 25µM) were used to confirm that purinergic and IL-17c-evoked Ca^{2+} transients were mediated *via* purinergic receptors. Caffeine (50mM) was used as a control to assess the functionality of OM slices under antagonists treatments (Hegg, and Lucero, 2006).

Electro-olfactogram (EOG) recording

EOG recordings were performed on the OM of 2 month old mice in an opened nasal cavity configuration as described earlier (François et al., 2016). The hemi-head was placed in a recording chamber under an upright Olympus SZ51 stereo microscope (Olympus, Rungis, France) equipped with a low magnification objective (0.8 to 4x) and two MX-160 micromanipulators (Siskiyou, Inc., Grants Pass, OR, USA). The hemi-head was kept under a constant flow of humidified filtered air (~1000 ml/min) delivered through a 9 mm glass tube. This tube was positioned 2 cm from the epithelial surface. Odour stimulations were performed by blowing air puffs (200 ms, 200 ml/min) through an exchangeable Pasteur pipette enclosed in the glass tube containing a filter paper impregnated with 20 µL of odorant (Sigma Aldrich, Saint-

Quentin Fallavier, France). Recordings were made with glass micropipettes of 4–5MΩ. Simultaneous EOG recordings of the responses evoked by heptanal (1:1000 in mineral oil) were recorded until their amplitudes stabilized, (i.e. at least 3 successive responses displaying the same amplitude), and the last response was selected as the reference. We focused on heptanal as it gives the best results in our recordings in mice, with signal ranging from 5 to 25 mV according to the dose used (François et al. 2016). One endoturbinate was treated by local application of the mucosal saline solution (45 mM KCl, 20 mM $KC_2H_3O_2$, 55 mM $NaCH_3SO_4$, 1 mM $MgSO_4$, 5 mM $CaCl_2$, 10 mM HEPES, 11 mM glucose, 50 mM mannitol, pH 7.4, 350 mOsm adjusted with mannitol (Negroni et al., 2012)), while the other endoturbinate received the tested molecule (1µg/mL IL-17c (n=8)) through constant diffusion from a glass micropipette of ~10µM diameter. Control and treated endoturbinates (II_b and IV) were systematically alternated from one mouse hemi-head to the other. Responses were recorded on both endoturbinates simultaneously every 3 min, for 30 min following local treatment. Analyses were performed off-line using Clampfit 9.2 (Axon Instruments). Peak amplitude following the drug application was normalized to peak amplitude of the control response prior to the treatment. Results are presented as mean ± standard error of the mean (SEM).

qPCR and molecular biology

Total RNA was extracted from OM primary culture cells using the Trizol method then treated with DNase I. OligodT first strand cDNA were synthesized from 5 µg total RNA by the Superscript II reverse transcriptase (Invitrogen) following the manufacturers recommendations. cDNA templates (5 µL) were added to a 15 µl reaction mixture containing 200 nM primers (sequences in **Table 1**) and SYBR Green

GoTaq® qPCR Master Mix (Promega, Charbonnieres, France). The expression levels of target genes were measured using the CFX Connect qPCR platform (BioRad, Hercules, CA, USA). A dissociation curve was carried out at the end of the PCR cycle to verify the efficiency of the primers to produce a single and specific PCR amplification. Quantification was achieved using the ΔΔCt method. Standard controls of specificity and efficiency of the qPCR assays were performed. The mRNA expression was normalized to the expression level of β-actin and an efficiency corrective factor was applied for each primer pair (François et al., 2016).

Statistical analysis

Data are expressed as mean ± standard error of the mean (SEM). Regarding the immunohistochemistry quantification, the investigator performing the quantification was blind to the treatment group during analysis. Statistical significance was assessed using non-parametric Mann-Whitney tests or one-way or two-way ANOVA followed by Bonferroni multiple comparison post-hoc tests (GraphPad Prism software, GraphPad software Inc., CA, USA). A probability value of $P \leq 0.05$ was set for significant differences.

Results

Expression and functionality of IL-17c receptors in the OM

To specify the distribution of IL-17c receptors (IL-17re and IL-17ra), we first performed *in situ* hybridization of IL-17re and immunofluorescent staining of IL-17ra, the specific receptor subunits for IL-17c (Song et al., 2011). IL-17re expression was found on the apical part of the sustentacular cells (SCs) and in axon bundles (Fig. **1A**). We also detected IL-17ra expression in the same part of the OM (Fig. **1B**). These data show that in the OM, the axon bundles of OSNs and SCs may be responsive to IL-17c.

We next examined the functionality of the IL-17c system in neonatal mice using calcium imaging on OM slices. Transient application of mouse recombinant IL-17c (IL-17c – 500ng/mL) evoked robust calcium rises in SCs body layer (Fig. **2A**). To compare the IL-17c evoked responses in SCs to the effect of a known SC modulator, we used ATP to generate a calcium increase in the SCs, as described previously (Hegg et al. 2003; Fig. **2B**). Given the similar response patterns observed with ATP and IL-17c (Fig. **2C**), we hypothesized that stimulation with IL-17c might induce ATP release. Therefore, we preincubated slices with purinergic receptors antagonists (PRA - suramin 100µM and PPADS 25µM ; (Hegg et al. 2003)) and then performed stimulations with ATP or IL-17c (Fig. **2B$_3$, A$_3$**). As expected, slices incubated with the purinergic receptors antagonists no longer respond to stimulation with ATP (Fig. **2B$_3$**). The preincubation of slices with PRA also specifically blocked the calcium increase mediated by IL-17c. The responsiveness of the OM slices after PRA treatment was assessed with 5 mM caffeine inducing calcium level rises in OM slices independently of the purinergic pathway (Hegg et al., 2009). As expected, caffeine elicited an increase in intracellular calcium in both OSNs and sustentacular cells

independently of the presence of purinergic antagonists (**Supplementary Data Figure 1**). These results show that acute application of IL-17c is likely to induce the ATP release by olfactory mucosa cells, which in turn increase intracellular calcium level.

We next explored if this process was still present in adult mice. As OM slices can only be performed on very young mice due to the solidity of the cranial bones, another technique was needed. We therefore used electro-olfactogram (EOG) recordings as a proxy to validate the functionality of the IL-17c system. EOG recordings reflect the responses of the OM to odorant stimulation (Scott, and Scott-Johnson, 2002), and ATP application on mice OM decreases odour sensitivity (Hegg et al. 2003; Hegg et Lucero 2006). If IL-17c induces the release of ATP from OM cells in adult mice, it should impact the odorant responses of the OM similarly as ATP application. Simultaneous EOG recordings of the responses evoked by heptanal were obtained from the endoturbinates IIb and IV (Fig. **3A**). One endoturbinate was treated by a local application of mucus solution (MS), while the other endoturbinate received the same MS containing IL-17c at 1µg/mL (Fig. **3A, B**). The evolution over time of the amplitude was significantly decreased following treatment with IL-17c compared to saline (Two-way ANOVA; $F_{(1,144)} = 5.66$; $P = 0.031$ Fig. **3C, D**). This decrease is consistent with a release of ATP induced by the presence of IL-17c.

Overall, our results show that the IL-17c system is functional on *ex vivo* preparations of the OM in neonatal and adult mice. They further suggest that IL-17c modulates calcium signalling indirectly *via* the release of ATP.

IL-17c increases cellular dynamics of the OM

After highlighting the functionality of the IL-17c in an *ex vivo* system, we decided to explore the impact of IL-17c on the OM *in vivo.* We thus examined whether the cellular dynamics of the OM was altered in mice intranasally instilled with IL-17c. As cellular dynamic of the olfactory epithelium is region dependent (Vedin et al., 2009), we studied the distribution of apoptosis, proliferation, and Iba1+ immune cells infiltration across the olfactory mucosa. In order to explore the effect of acute and chronic treatment with IL-17c, we performed intranasal instillations of IL-17c for one day and one week, respectively.

We first examined the effect of a single IL-17c administration on the OM dynamics. 24h after this nasal instillation, we did not observe any significant modification of the cellular dynamic of the epithelium in terms of apoptosis (Mann-Whitney; P = 0.519 ; P = 0.774 ; P = 0.628 in caudal, medial and rostral area respectively), cell proliferation (P = 0.533 ; P = 0.731 ; P = 0.295 in caudal, medial and rostral area respectively) and immune cell infiltrations (P = 0.534 ; P = 0.366 ; P = 0.234 in caudal, medial and rostral area respectively) (**Supplementary Figure 2**). However, we observed a significant increase of cleaved caspase 3 signal, (major component of the apoptosis signalling pathway) in one week treated IL-17c mice compared to the untreated control group. This increase was present in medial and rostral areas of the OM (Fig. **4A$_1$**; Mann Whitney; P = 0.022 and 0.014, respectively). We next examined the OM proliferation rate by immunohistochemistry raised against PCNA (a scaffold protein involved in DNA replication; (François et al., 2016)) and also observed a significant increase of PCNA staining in the rostral area (Fig. **4B$_1$**; Mann Whitney; P = 0.002). We finally examined the immune Iba1+ cell infiltration (specific marker of monocyte/macrophage lineage, (Hasegawa-Ishii et al., 2017) in the OM. Treatment

with IL-17c led to an increase of immune cells infiltration in the OM in its medial and rostral areas (Fig. **4C$_1$**; Mann Whitney; both P = 0.035).

Overall, these results indicate that the cellular turn-over in the OM is increased in IL-17c treated mice and that several days of IL-17c treatment trigger an immune cell infiltration in the OM.

IL-17c is induced *in vivo* in the OM following Poly(I:C) stimulation mimicking virus presence

Under physiological conditions, IL-17c is expressed at a very low level in the OM according to our *in situ hybridization* and qPCR experiments. As the receptors to IL-17c are strongly expressed in the OM, we next hypothesized that IL-17c may be released under specific situations like inflammation following bacterial or viral stimuli as shown for respiratory epithelium cells *in vitro* (Pfeifer et al., 2013). Polyinosinic:polycytidylic acid (Poly(I:C) is structurally similar to double-stranded RNA present in part of the RNA virus family and is used experimentally to model viral infections *in vivo* (Kanaya et al., 2014). Furthermore, Poly(I:C) is a potent inducer of IL-17c in primary airway epithelial cells according to *in vitro* studies (Kusagaya et al., 2013; Pfeifer et al., 2013). We performed intranasal administration of Poly(I:C) similarly as a previous study on the innate immune responses of the OM (Kanaya et al. 2014 - Fig. **5**). After a 3-day treatment, we observed degenerative changes of the olfactory area treated with Poly(I:C) (Fig. **5C**). Degeneration was characterized by detachment of the neuroepithelium from the basal lamina (Fig. **5C$_3$**) and was absent in the contralateral, non-treated OM (Fig. **5C$_2$**). Intranasal instillations of Poly(I:C) also induced a strong expression of IL-17c in the whole olfactory epithelium, the nasal-associated lymphoid tissue (NALT) and particularly in the Steno's gland (also

known as lateral nasal gland ; Fig. **5D**). The IL-17c expression followed the time course of Poly(I:C) treatment and decreased after the end of Poly(I:C) nasal instillations at D7 (One way ANOVA analysis followed by Bonferroni's Multiple Comparison Test; $P < 0.001$; Fig. **5B**). Together, these results indicate that IL-17c is mainly expressed locally *in vivo* in the OM, NALT and lateral nasal gland under a Poly(I:C) challenge.

Intranasal instillation of IL-17C results in a decrease of expression of tight junction related proteins

Nasal administration of Poly(I:C) led concomitantly to a disturbance of OM integrity and to an increase in IL-17c expression. As IL-17c plays a critical role in intestinal mucosal barrier integrity (Reynolds et al., 2012), we evaluated a potential involvement of IL-17c in OM barrier stability. As we previously observed that ATP was likely released from OM cells in the presence of IL-17c (Fig. **2**), we also evaluated if ATP could also be involved in this process. The observed shedding of the OM neuroepithelium (Fig. **5C$_3$**) in mice treated with Poly(I:C), was absent in mice treated with vehicle (Fig. **5C$_2$**), IL-17c (Fig. **5C$_4$**) or ATP (Fig. **5C$_5$**). We thus compared the effects of Poly(I:C), IL-17c, and ATP delivered intranasally on the expression of genes related to barrier integrity. We measured the expression of genes related to tight junction in the OM (claudin 1, claudin 11 and tight junction protein 1 – TJP1 (Steinke et al., 2008; Krishan et al., 2014)). As expected (Kanaya et al., 2014; Huang et al., 2016; Gon et al., 2016), the expression of genes related to tight junction formation was reduced in olfactory mucosa of Poly(I:C) treated-mice: claudin 1 (Fig. **6A$_1$**; Mann Whitney; $P = 0.023$), claudin 11 (Fig. **6A$_2$**; $P = 0.028$) and TJP1 (Fig. **6A$_3$**; $P = 0.006$). With regards to IL-17c, intranasal treatment also resulted

in a decrease of expression of claudin 1 (Fig. **6A$_1$**; P = 0.007), claudin 11 (Fig. **6A$_2$**; P = 0.003) and TJP1 (Fig. **6A$_3$**; P = 0.046). Interestingly, the expression of various tight junction proteins remained unchanged between vehicle and ATP-treated mice (Fig. **6A** - claudin 1, P = 0.681; claudin 11, P = 0.147 and TJP1, P = 0.244).

Overall, our results suggest that IL-17c decreases the permeability of the neuroepithelium as indicated by changes in the tight junction genes expression.

Pretreatment and cotreatment with IL-17c modulate cell death induced by Poly(I:C) treatment of OM primary culture

IL-17c is a neurotrophic cytokine that protects peripheral nerve systems during HSV reactivation *in vitro* (Peng et al., 2017). We explored its protective role in a primary culture model. We selected the *in vitro* model for its reliability, as compared to the variability observed *in vivo* and to avoid the endogenous production of IL-17c. We tested if pretreatment with IL-17c could improve the cellular survival of a primary culture of OM during a Poly(I:C) challenge. Seven days after *in vitro* development of the culture, primary culture of the OM were treated with Poly(I:C) alone or with IL-17c (Fig. **7A**). The level of cellular death was then evaluated by the LDH released from dying cells one week after the treatments. The level of cellular death was increased following Poly(I:C) treatment (Fig. **7B**; Mann Whitney; P < 0.001) while the treatment with IL-17c alone did not affect LDH release (Fig. **7B**; P = 0.611). Pretreatment or co-treatment with IL-17c of cell treated with Poly(I:C) led to a significant decrease of LDH release (Fig **7B**; P < 0.001).

Discussion

Due to its position at the interface between environment and central nervous system, the olfactory mucosa is an immunologically sensitive site. While OM studies are focused on odorant detection, it is also a place of synthesis and secretion of antimicrobial and immunological compounds (Mellert et al., 1992). However, very few defence mechanisms are described and the interaction of the immunity actors within the OM remains to be explored (Chen et al., 2017). Similarly, there is an important body of literature for peripheral modulation of odorant detection (Lucero, 2013) but very few papers focus on the potent neuromodulator effects of immune compounds despite the growing evidence on neuromodulatory properties of cytokines (Vezzani, and Viviani, 2015). Previous findings on primary normal human bronchial epithelial cells suggest a pivotal role of IL-17c in the respiratory epithelium (Kusagaya et al., 2013; Pfeifer et al., 2013). Indeed, in these studies, Poly(I:C) treatment induced IL-17c expression *via* the Toll-like receptor 3, and IL-17c enhanced mucosal host defence responses *via* a unique autocrine/paracrine manner. In our study, we explored IL-17c presence, production and functionality on the olfactory mucosa.

We first report that IL-17c receptors are expressed in the OM by *in situ* hybridization and immunohistochemical approaches (**Fig. 1**). The distribution patterns of IL-17re and IL-17ra show the presence of receptors in SCs and in axonal bundles of OSNs. The expression of IL-17c receptors in axonal parts of neurons is consistent with a previous study showing that IL-17c receptors are present in sensory neurons from human foetal dorsal root ganglia (Peng et al., 2017). Together these results highlight the expression of IL-17c receptors in two immunologically sensitive sites as sustentacular cells are directly exposed to airborne substances (Makino et al., 2009;

Kanaya et al., 2014) and axonal bundles connect the environment to the central nervous system.

The expression of IL-17c was reported in transcriptomic studies (Ibarra-Soria et al., 2014; Kanageswaran et al., 2015). Our qPCR and *in situ hybridization* results on control animals indicate that the basal level of IL-17c expression in the Steno's gland and in the OM is very low. However, its expression was induced by *in vivo* intranasal instillation of Poly(I:C) in a time-dependent manner. The IL-17c expression follows the time course of Poly(I:C) treatment and decreases after the end of the treatment. IL-17c was mainly expressed in lateral nasal glands (LNG – also known as Steno's gland; **Fig. 5**), which are described as an important site of secretion of mucus components within the nasal cavity (Badonnel et al., 2009). The LNG, even if poorly described in the literature, are believed to act as an immune barrier through secretion of immunoglobulin A (Mellert et al., 1992) and their expression of IL-17c supports a role in immunity for this gland. IL-17c is also induced by Poly(I:C) treatment *in vivo.* As we observed that IL-17c is active in the OM, our results are in agreement with previous evidences of autocrine and paracrine action of IL-17c (Kusagaya et al., 2013).

Functionally, we observed that IL-17c modulates the calcium levels within seconds of application *ex vivo*. A transduction pathway of cytokines linked to calcium level increase is rather unusual but has been observed with IL-1β in several models of primary culture (cortical astrocytes, hypothalamus neurons and area postrema cells - Holliday et Gruol 1993; De et al. 2002; Wuchert et al. 2009). We observed a very similar cellular pattern of activation between IL-17c and ATP used as a positive control. We hypothesized that the Ca^{2+} level rise induced by IL-17c application could be indirect through the release of ATP. Such mechanism has already been observed

with IL-1β inducing ATP release in rat hippocampal slices (Sperlágh et al., 2004). In our study, IL-17c responses were effectively blocked by purinergic receptors antagonists supporting a similar mechanism of action for IL-17c (**Fig. 2**). As these experiments were performed on slices from mice pups, we wanted to confirm it in adult mice. Unfortunately, the robustness of adult mice bones prevent an approach using OM slices. ATP has been previously characterized for its ability to reduce the odour-induced responses in mice (Hegg et al., 2003; Lucero, 2013). If IL-17c leads to a release of ATP in adult mice, its application in the OM should also decrease the response to odorant stimulations. Our EOG results show that IL-17c decrease the amplitude of odour induced response in the OM. Overall, our results are consistent with an IL-17c-induced ATP release in mice.

We next examined how exogenous murine recombinant IL-17c nasal instillation impacts the cellular turn-over of OM. A single instillation of IL-17c had no effect in terms of apoptosis, cell proliferation or Iba1+ cell infiltrations. However, we observed that repeated administration of IL-17c promoted both apoptosis and proliferation, suggesting a role in the cellular dynamics of the OM (**Fig. 4)**. In addition to the cellular dynamic modulation, we also observed that IL-17c led to macrophage/microglia-like cell infiltration in the olfactory mucosa. Similarly, IL-17c was shown to promote the recruitment of immune cells around smooth muscle cells in mice (Butcher et al., 2016). Therefore, IL-17c may act *in vivo* as a chemotactic compound in the OM. The infiltration of Iba1+ cells may explain the increase in cellular dynamics of the OM in our chronic model. Indeed, recruitment of macrophages will lead to the establishment of an inflammatory state modulating neuronal survival and basal cell proliferation (Borders et al., 2007a; Borders et al., 2007b). Additionally, as ATP promotes cell proliferation in the OM (Jia et al., 2011),

the OM cellular proliferation induced by IL-17c may rely in part, on the ATP release induced by IL-17c.

Poly(I:C) nasal instillation led to morphological changes of the OM (**Fig. 5**). This nasal instillation also increased the IL-17c expression level and we examined the importance of IL-17c for the OM morphological changes induced by Poly(I:C) treatment. Similarly as Poly(I:C), IL-17c instillation led to a decrease of the expression of genes related to the neuroepithelium barrier but without alteration of the epithelium morphology (**Fig. 5, 6**). Furthermore, this effect did not rely on ATP release induced by IL-17c treatment as nasal instillation of ATP did not modify tight junction protein expression. This last result shows that IL-17c impacts the OM physiology not only through ATP release. Our results of the effect of IL-17c on the OM barrier integrity contrast with its impact on colonic epithelial cells where it promotes tight junction genes expression (Reynolds et al., 2012). However, cytokines can increase or decrease the expression of tight junction proteins depending on the organ (Capaldo, and Nusrat, 2009).

A recent study highlighted a protective role of IL-17c in the peripheral nervous system (Peng et al., 2017). We choose to explore a similar role of IL-17c during a Poly(I:C) challenge in the OM. As IL-17c was induced by Poly(I:C) *in vivo*, we used a primary culture of OM cells allowing a control of the extracellular medium and thus of IL-17c concentration. In this culture, while Poly(I:C) increased the level of cellular death, co and pre-treatment with IL-17c improved the survival of OM cells (**Fig. 7**). This last result contrasts with the *in vivo* treatment where IL-17c nasal instillation led to an increase in apoptosis level. The simplest explanation for this discrepancy would be that the up regulation of cell turnover observed *in vivo* is triggered by the macrophage/monocyte infiltration induced by the administration of IL-17c. As those

cells are not present in the primary culture, we could observe an anti-apoptotic effect of IL-17c.

Overall, our results show that IL-17c can increase the cellular dynamic of the OM toward regeneration. Such action would help to counterbalance the massive damages observed after viral infection of the olfactory mucosa leading to post viral olfactory disorders (Kanaya et al., 2014). The olfactory bulb is often considered as the first barrier against airborne pathogens entry to the central nervous system (Durrant et al., 2016). As several other cytokines receptors are expressed in the OM (Ibarra-Soria et al., 2014; Saraiva et al., 2016), our results indicate that before the olfactory bulb line of defences, the OM could be an effective barrier against airborne pathogens.

Acknowledgment:

This work was funded by the Institut National de la Recherche Agronomique (INRA). We would like to thank Birte Nielsen for her help improving the manuscript, Patrice Dahirel and Aurélien Raynaud for animal care and treatments; Audrey Prézelin, Christian Ouali and Marie Annick Persuy for technical help.

Conflict of interests:

The authors declare no conflict of interests.

Author contributions:

BB and NM designed, performed experiments, analysed data and wrote the paper, AD performed experiments and analysed the data, CLPS and AS performed experiments; PC designed and performed experiments.

Andersen I, Lundqvist GR, Proctor DF (1971): Human nasal mucosal function in a controlled climate. Arch Environ Health 23:408–420.

Antunes MB, Cohen NA (2007): Mucociliary clearance--a critical upper airway host defense mechanism and methods of assessment. Curr Opin Allergy Clin Immunol 7:5–10.

Badonnel K, Durieux D, Monnerie R, Grébert D, Salesse R, Caillol M, et al. (2009): Leptin-sensitive OBP-expressing mucous cells in rat olfactory epithelium: a novel target for olfaction-nutrition crosstalk? Cell Tissue Res 338:53–66.

Borders AS, Getchell ML, Etscheidt JT, van Rooijen N, Cohen DA, Getchell TV (2007a): Macrophage depletion in the murine olfactory epithelium leads to increased neuronal death and decreased neurogenesis. J Comp Neurol 501:206–218.

Borders AS, Hersh MA, Getchell ML, van Rooijen N, Cohen DA, Stromberg AJ, et al. (2007b): Macrophage-mediated neuroprotection and neurogenesis in the olfactory epithelium. Physiol Genomics 31:531–543.

Butcher MJ, Waseem TC, Galkina EV (2016): Smooth muscle cell-derived IL-17C plays an atherogenic role *via* the recruitment of pro-inflammatory IL-17A+ T cells to the aorta. Arterioscler Thromb Vasc Biol 36:1496–1506.

Capaldo CT, Nusrat A (2009): Cytokine regulation of tight junctions. Biochim Biophys Acta BBA - Biomembr 1788:864–871.

Chang SH, Reynolds JM, Pappu BP, Chen G, Martinez GJ, Dong C (2011): Interleukin-17C Promotes Th17 Cell Responses and Autoimmune Disease via Interleukin-17 Receptor E. Immunity 35:611–621.

Chen M, Reed RR, Lane AP (2017): Acute inflammation regulates neuroregeneration through the NF-κB pathway in olfactory epithelium. Proc Natl Acad Sci U S A 114:8089–8094.

Dando SJ, Mackay-Sim A, Norton R, Currie BJ, St. John JA, Ekberg JAK, et al. (2014): Pathogens Penetrating the Central Nervous System: Infection Pathways and the Cellular and Molecular Mechanisms of Invasion. Clin Microbiol Rev 27:691–726.

De A, Churchill L, Obal F, Simasko SM, Krueger JM (2002): GHRH and IL1β increase cytoplasmic Ca^{2+} levels in cultured hypothalamic GABAergic neurons. Brain Res 949:209–212.

Durrant DM, Ghosh S, Klein RS (2016): The Olfactory Bulb: An Immunosensory Effector Organ during Neurotropic Viral Infections. ACS Chem Neurosci 7:464–469.

François A, Grebert D, Rhimi M, Mariadassou M, Naudon L, Rabot S, et al. (2016): Olfactory epithelium changes in germfree mice. Sci Rep 6. DOI: 10.1038/srep24687

François A, Laziz I, Rimbaud S, Grebert D, Durieux D, Pajot-Augy E, et al. (2013): Early survival factor deprivation in the olfactory epithelium enhances activity-driven survival. Front Cell Neurosci 7. DOI: 10.3389/fncel.2013.00271

Gänger S, Schindowski K (2018): Tailoring Formulations for Intranasal Nose-to-Brain Delivery: A Review on Architecture, Physico-Chemical Characteristics and Mucociliary Clearance of the Nasal Olfactory Mucosa. Pharmaceutics 10. DOI: 10.3390/pharmaceutics10030116

Gon Y, Maruoka S, Kishi H, Kozu Y, Kuroda K, Mizumura K, et al. (2016): DsRNA disrupts airway epithelial barrier integrity through down-regulation of claudin members. Allergol Int 65:S56–S58.

Gouadon E, Meunier N, Grebert D, Durieux D, Baly C, Salesse R, et al. (2010): Endothelin evokes distinct calcium transients in neuronal and non-neuronal cells of rat olfactory mucosa primary cultures. Neuroscience 165:584–600.

Gu C, Wu L, Li X (2013): IL-17 family: Cytokines, receptors and signaling. Cytokine 64:477–485.

Hanson LR, Fine JM, Svitak AL, Faltesek KA (2013): Intranasal Administration of CNS Therapeutics to Awake Mice. J Vis Exp JoVE DOI: 10.3791/4440

Hasegawa-Ishii S, Shimada A, Imamura F (2017): Lipopolysaccharide-initiated persistent rhinitis causes gliosis and synaptic loss in the olfactory bulb. Sci Rep 7. DOI: 10.1038/s41598-017-10229-w

Hegg CC, Greenwood D, Huang W, Han P, Lucero MT (2003): Activation of Purinergic Receptor Subtypes Modulates Odor Sensitivity. J Neurosci Off J Soc Neurosci 23:8291–8301.

Hegg CC, Irwin M, Lucero MT (2009): Calcium store-mediated signaling in sustentacular cells of the mouse olfactory epithelium. Glia 57:634–644.

Hegg CC, Lucero MT (2006): Purinergic receptor antagonists inhibit odorant-induced heat shock protein 25 induction in mouse olfactory epithelium. Glia 53:182–190.

Holliday J, Gruol DL (1993): Cytokine stimulation increases intracellular calcium and alters the response to quisqualate in cultured cortical astrocytes. Brain Res 621:233–241.

Huang L-Y, Stuart C, Takeda K, D'Agnillo F, Golding B (2016): Poly(I:C) Induces Human Lung Endothelial Barrier Dysfunction by Disrupting Tight Junction Expression of Claudin-5. PloS One 11:e0160875.

Ibarra-Soria X, Levitin MO, Saraiva LR, Logan DW (2014): The Olfactory Transcriptomes of Mice. PLoS Genet 10:e1004593.

Jia C, Sangsiri S, Belock B, Iqbal TR, Pestka JJ, Hegg CC (2011): ATP Mediates Neuroprotective and Neuroproliferative Effects in Mouse Olfactory Epithelium

following Exposure to Satratoxin G. In Vitro and In VivoToxicol Sci 124:169–178.

Kanageswaran N, Demond M, Nagel M, Schreiner BSP, Baumgart S, Scholz P, et al. (2015): Deep Sequencing of the Murine Olfactory Receptor Neuron Transcriptome. PLOS ONE 10:e0113170.

Kanaya K, Kondo K, Suzukawa K, Sakamoto T, Kikuta S, Okada K, et al. (2014): Innate immune responses and neuroepithelial degeneration and regeneration in the mouse olfactory mucosa induced by intranasal administration of Poly(I:C). Cell Tissue Res 357:279–299.

Krishan M, Gudelsky GA, Desai PB, Genter MB (2014): Manipulation of olfactory tight junctions using papaverine to enhance intranasal delivery of gemcitabine to the brain. Drug Deliv 21:8–16.

Kusagaya H, Fujisawa T, Yamanaka K, Mori K, Hashimoto D, Enomoto N, et al. (2013): TLR-Mediated Airway IL-17C Enhances Epithelial Host Defense in an Autocrine/Paracrine MannerAm J Respir Cell Mol Biol :130814091442000.

Laziz I, Larbi A, Grebert D, Sautel M, Congar P, Lacroix MC, et al. (2011): Endothelin as a neuroprotective factor in the olfactory epithelium. Neuroscience 172:20–29.

Le Bourhis M, Rimbaud S, Grebert D, Congar P, Meunier N (2014): Endothelin uncouples gap junctions in sustentacular cells and olfactory ensheathing cells of the olfactory mucosa. Eur J Neurosci 40:2878–2887.

Lucero MT (2013): Peripheral modulation of smell: fact or fiction? Semin Cell Dev Biol 24:58–70.

Makino N, Ookawara S, Katoh K, Ohta Y, Ichikawa M, Ichimura K (2009): The morphological change of supporting cells in the olfactory epithelium after bulbectomy. Chem Senses 34:171–179.

Mellert TK, Getchell ML, Sparks L, Getchell TV (1992): Characterization of the immune barrier in human olfactory mucosa. Otolaryngol--Head Neck Surg Off J Am Acad Otolaryngol-Head Neck Surg 106:181–188.

Negroni J, Meunier N, Monnerie R, Salesse R, Baly C, Caillol M, et al. (2012): Neuropeptide Y Enhances Olfactory Mucosa Responses to Odorant in Hungry Rats. PLoS ONE 7:e45266.

Pägelow D, Chhatbar C, Beineke A, Liu X, Nerlich A, Vorst K van, et al. (2018): The olfactory epithelium as a port of entry in neonatal neurolisteriosis. Nat Commun 9:4269.

Peng T, Chanthaphavong RS, Sun S, Trigilio JA, Phasouk K, Jin L, et al. (2017): Keratinocytes produce IL-17c to protect peripheral nervous systems during human HSV-2 reactivation. J Exp Med 214:2315–2329.

Pfeifer P, Voss M, Wonnenberg B, Hellberg J, Seiler F, Lepper PM, et al. (2013): IL-17C Is a Mediator of Respiratory Epithelial Innate Immune Response. Am J Respir Cell Mol Biol 48:415–421.

Reynolds JM, Martinez GJ, Nallaparaju KC, Chang SH, Wang Y-H, Dong C (2012): Cutting Edge: Regulation of Intestinal Inflammation and Barrier Function by IL-17C. J Immunol 189:4226–4230.

Saraiva LR, Ibarra-Soria X, Khan M, Omura M, Scialdone A, Mombaerts P, et al. (2016): Hierarchical deconstruction of mouse olfactory sensory neurons: from whole mucosa to single-cell RNA-seq. Sci Rep 5. DOI: 10.1038/srep18178

Scott JW, Scott-Johnson PE (2002): The electroolfactogram: a review of its history and uses. Microsc Res Tech 58:152–160.

Song X, Zhu S, Shi P, Liu Y, Shi Y, Levin SD, et al. (2011): IL-17RE is the functional receptor for IL-17C and mediates mucosal immunity to infection with intestinal pathogens. Nat Immunol 12:1151–1158.

Sperlágh B, Baranyi M, Haskó G, Vizi ES (2004): Potent effect of interleukin-1β to evoke ATP and adenosine release from rat hippocampal slices. J Neuroimmunol 151:33–39.

Steinke A, Meier-Stiegen S, Drenckhahn D, Asan E (2008): Molecular composition of tight and adherens junctions in the rat olfactory epithelium and fila. Histochem Cell Biol 130:339–361.

Vedin V, Molander M, Bohm S, Berghard A (2009): Regional differences in olfactory epithelial homeostasis in the adult mouse. J Comp Neurol 513:375–384.

Vezzani A, Viviani B (2015): Neuromodulatory properties of inflammatory cytokines and their impact on neuronal excitability. Neuropharmacology 96:70–82.

Wuchert F, Ott D, Rafalzik S, Roth J, Gerstberger R (2009): Tumor necrosis factor-α, interleukin-1β and nitric oxide induce calcium transients in distinct populations of cells cultured from the rat area postrema. J Neuroimmunol 206:44–51.

Figure 1: Expression of IL-17c receptors in the mouse olfactory mucosa. (**A**) In situ hybridization of IL-17re and (**B**) immunohistochemistry of IL-17ra indicate that both IL-17c receptors subunits are mainly expressed in the apical part of the olfactory epithelium corresponding to sustentacular cells and in axon bundles of the lamina propria.

Figure 2: IL-17c mediates a rise in calcium in sustentacular cells and in neurons through the release of ATP. Representative calcium wave spreading before (**A_1**, **B_1**) and after IL-17c (**A_2**) or ATP (**B_2**). Stimulation of slices preincubated in presence of purinergic receptors antagonists ("PRA" -suramin (100µM), PPADS (25µM - **A_3; B_3**) or not (**A_2**, **B_2**)). (**C**) Average time courses of the effect of ATP (10^{-4} M), IL-17c (500ng/mL) on the calcium signal measured in the ROI containing the SCs layer. Drug application starts at the black arrow and lasts 30s ($\Delta F/F \pm$ SEM; n=5 per condition).

Figure 3: Amplitude of olfactory response is diminished by IL-17c treatment. (**A**) Schematic diagram of the experimental preparation allowing the simultaneous recording of two OM areas treated with saline and IL-17c (1µg/mL) respectively. EOG recordings were performed on endoturbinates IIb and IV located centrally in the nasal cavity. (**B**) Time course of recordings and treatments (**C**) Effects of treatment on the time course of normalized EOG amplitudes in response to heptanal (1:1000 in mineral oil). Mean ± SEM values are expressed as % of control EOG recordings prior to treatment (n=9). Two way ANOVA (*P<0.05). (**D**) Typical normalized EOG responses to heptanal (1:1000 in mineral oil) before and 20 minutes after treatment.

Figure 4: Cellular dynamics of the OM is enhanced in mice intranasally instilled with IL-17c. The cellular dynamic of the OM was evaluated by quantifying the areas with cleaved caspase 3 (C3C; (**A**)), proliferating cell nuclear antigen (PCNA; (**B**)) and the number of cell stained against ionized calcium-binding adapter molecule 1 (Iba1+; (**C**)), taken as indices of apoptosis, proliferation and infiltration of monocyte/macrophage cells, respectively. Results were expressed as mean of the C3C and PCNA signal area and Iba1+ cells counts in the OM in each region of interest (n=6 vehicle-treated mice / n=7 IL-17c (500ng/mL) treated mice). Representative images of (**A2-3**) C3C staining with OSN ongoing apoptosis, (**B2-3**) PCNA staining mainly present in basal cell and (**C2-3**) Iba1+ staining.

Figure 5: Expression of IL-17c in a pseudo-viral context induced by Poly(I:C) (**A**) Experimental protocol for intranasal administration of Poly(I:C) (20 µg Poly(I:C) sodium salt dissolved in 10 µL of sterile saline into each nostril) or vehicle. Mice received a maximum of five intranasal administrations of Poly(I:C) or vehicle solution, once every 24 h, and were sacrificed 3, 5 or 7 days after the first administration (n = 8,8,6 respectively). Control mice were also sacrificed at 3, 5 and 7 days after the first vehicle administration (n=9). (**B**) Dot plot of the mRNA relative level of IL-17c concentration for individual mice expressed in the OM. The expression level was normalized to β-actin and is presented as mean ± SEM. Different letters represent significantly different groups. (**C**) Hematoxylin *and* eosin staining of representative OMs from a mouse treated unilaterally with Poly(I:C). Panels show details of olfactory mucosa of mice nasally instilled with vehicle (**C_2**)**,** Poly(I:C) (**C_3**), IL-17c (500ng/mL) **C_4**) or ATP (10^{-4}M) (**C_5**). (**D**) Representative image with light microscopy of IL-17c mRNA expression in a D-5 treated mouse visualized by *in situ* hybridization with sense and antisense probe. Panels on the right show details of Steno's gland (**D_2, D_3**), olfactory mucosa (**D_4, D_5**) and nasal associated lymphoid tissue (**D_6, D_7**). The zone with the sense probe as a control is on the left (**D_2**, **D_4**, **D_6**).

Figure 6: Intranasal instillation of IL-17C results in a decrease in expression of tight junction related proteins. Mice accustomed to receive intranasal instillations receive a three day treatment of vehicle (Ctrl), Poly(I:C) (2g/L), IL-17C (500ng/mL) or ATP (10^{-4}M); n=13, 9, 16, 13 respectively. The mRNA level of tight junction related proteins (claudin-1 (**A**), claudin-11 **(B)** or tight junction protein-1 **(C)** was further evaluated by quantification on cDNAs from olfactory mucosa by real time RT-PCR. Their expression levels were normalized to that of β-actin and are given as mean ± SEM. Different letters represent significantly different groups.

Figure 7: Anti-cytotoxic effect of IL-17c in a primary culture of OM during a Poly(I:C) challenge. (**A**) Experimental design. The OM primary culture was grown for 7 days before supplementation with culture medium alone (control) or containing Poly(I:C) (1mg/mL) and/or IL-17c (200ng/mL). The impact of these various treatments on cell death in the OM primary culture was quantified by the percentage of LDH released in the extracellular medium. (**B**) Dot plot representing the relative LDH released in presence of various treatments including co-treatment ("Co" Poly(I:C) - IL-17c) and pre-treatment with IL-17c ("Pre"). The relative LDH release was estimated by measuring the cellular LDH content and expressed as a relative value to the control condition. Data are presented as mean ± SEM (n=16 per condition). Columns with different letters differ significantly.

Table 1. Primers used for qPCR reactions

	GenBank Accession number	Sequences primers (5'>3')	Tm (°C)
β- actin	NM_007393.5	GACCCAGATCATGTTTGAGACCTT	60.57
		CACAGCCTGGATGGCTACGT	62.24
Claudin-1	NM_016674.4	ACTGTGGATGTCCTGCGTTT	59.89
		CCCCAGCAGGATGCCAATTA	60.11
Claudin-11	NM_008770.3	ACATCCTCATCCTTCCAGGCTA	60.36
		ATGCAGGGGAGAACTGTCAA	58.93
Tight Junction Protein 1	NM_009386	GGAGATGTTTATGCGGACGG	58.78
		CCATTGCTGTGCTCTTAGCG	59.62
IL-17c	NM_145834.4	CTGGAAGCTGACACTCACGA	59.68
		CCACGACACAAGCATTCTGC	60.11

Supplementary Figure 1: Caffeine mediates a rise in calcium rise in sustentacular cells and in neurons in the presence of purinergic antagonists receptors. Representative calcium wave spreading with caffeine (50nM) before (caffeine) or after (caffeine + antagonists) the incubation with purinergic antagonist receptors. Average time courses of the effect of caffeine on the calcium signal measured in the ROI containing the SCs/OSNs layer. Drug application starts at the black arrow and lasts 30s ($\Delta F/F \pm SEM$; n=4).

Supplementary Figure 2: Cellular dynamics of the OM is not altered 24h after unique nasal instillation of IL-17c. The cellular dynamic of the OM was evaluated by quantifying the areas with cleaved caspase 3 (C3C; (**A**)), proliferating cell nuclear antigen (PCNA; (**B**)) and the number of cell stained against ionized calcium-binding adapter molecule 1 (Iba1+; (**C**)), taken as indices of apoptosis, proliferation and infiltration of monocyte/macrophage cells, respectively. Results were expressed as mean of the C3C and PCNA signal area and Iba1+ cells counts in the OM in each region of interest (n=6 vehicle-treated mice / n=7 IL-17c (500ng/mL) treated mice).

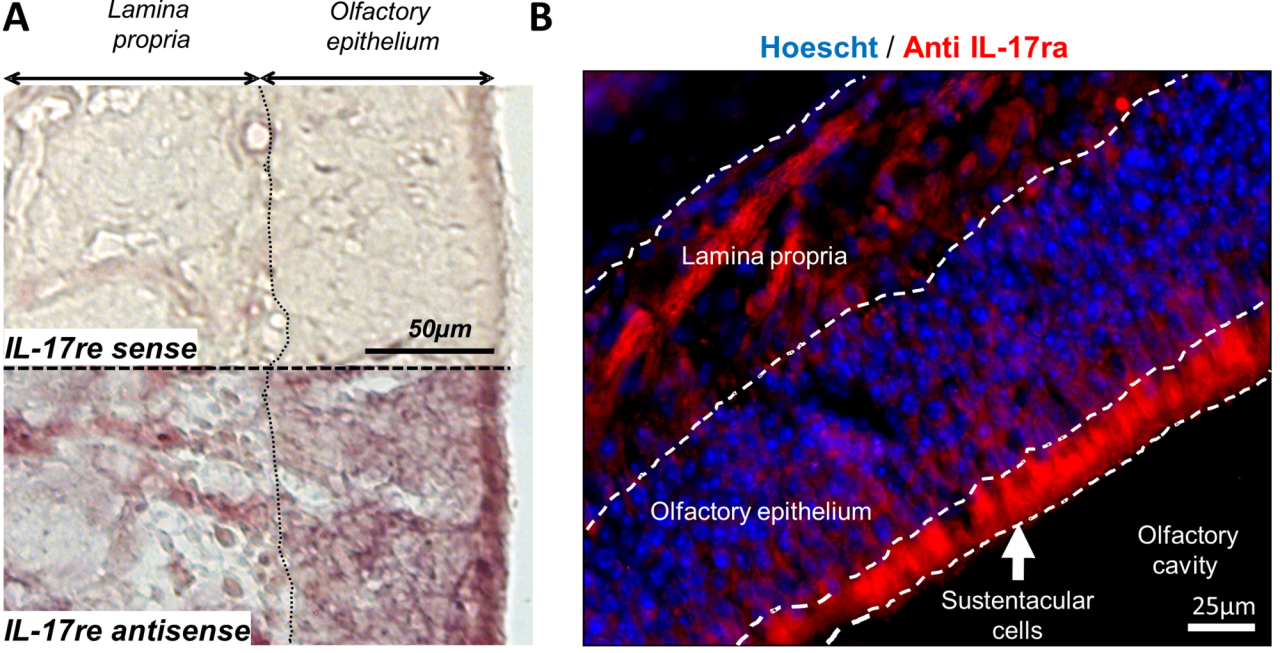
A
Lamina propria
Olfactory epithelium
50μm
IL-17re sense
IL-17re antisense
B
Hoescht / Anti IL-17ra
Lamina propria
Olfactory epithelium
Olfactory cavity
Sustentacular cells
25μm

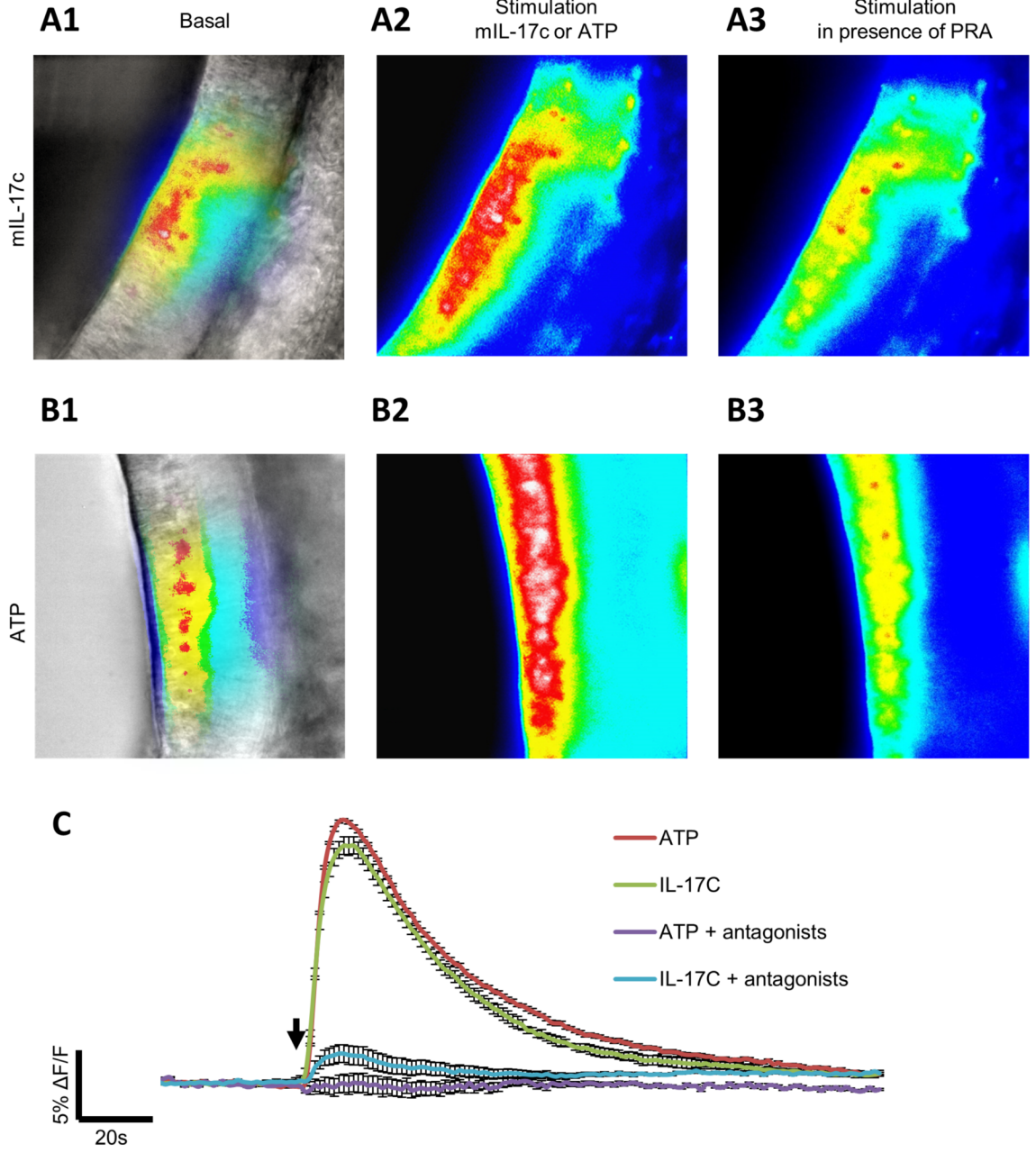
A1
Basal
A2
Stimulation
mIL-17c or ATP
A3
Stimulation
in presence of PRA
mIL-17c
B1
B2
B3
ATP
C
ATP
IL-17C
ATP + antagonists
IL-17C + antagonists
5% ΔF/F
20s

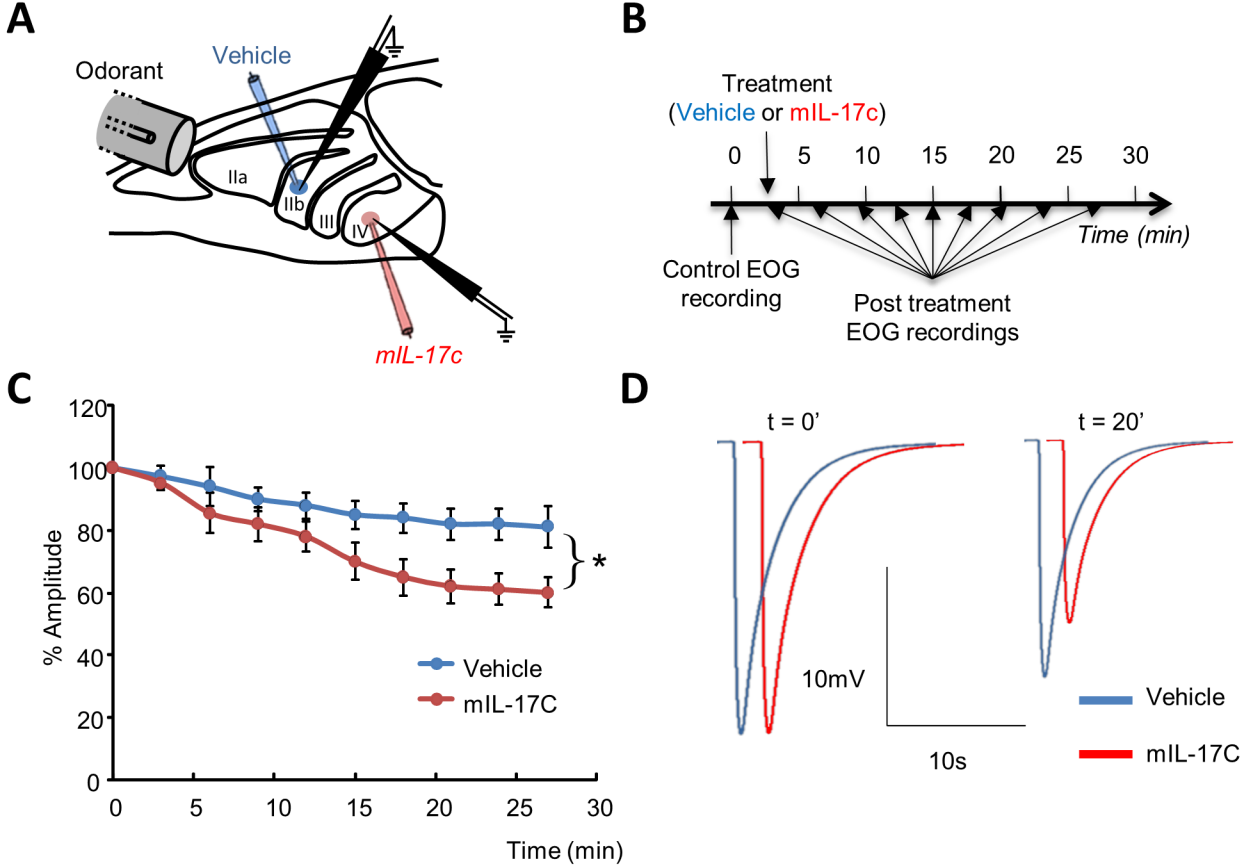
A
Odorant
Vehicle
IIa
IIb
III
IV
mIL-17c
B
Treatment
(Vehicle or mIL-17c)
0
5
10
15
20
25
30
Time (min)
Control EOG recording
Post treatment EOG recordings
C
% Amplitude
120
100
80
60
40
20
0
0
5
10
15
20
25
30
Time (min)
*
Vehicle
mIL-17C
D
t = 0'
t = 20'
10mV
10s
Vehicle
mIL-17C

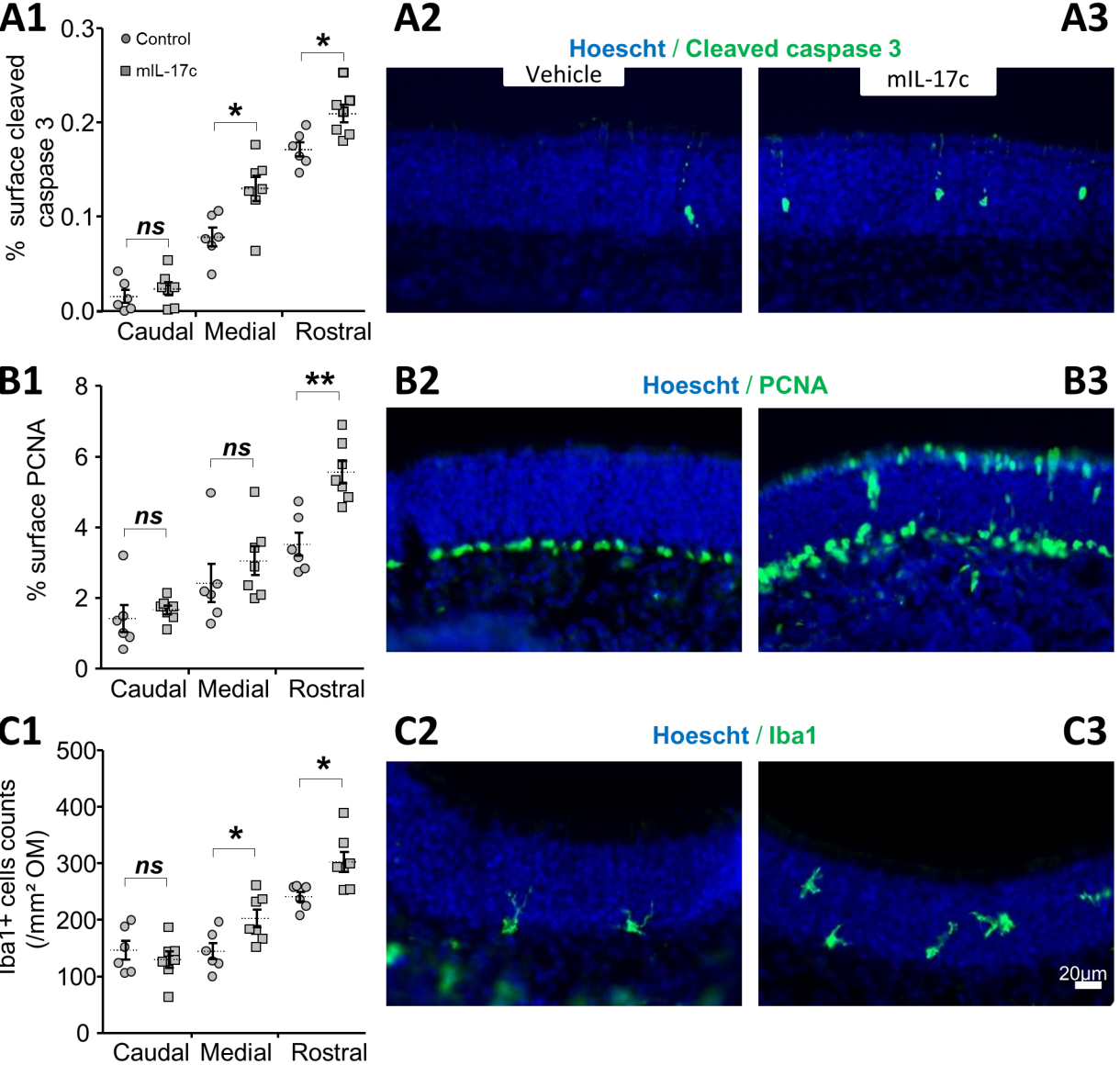
A1
A2
A3
Hoescht / Cleaved caspase 3
Vehicle
mIL-17c
% surface cleaved caspase 3
Control
mIL-17c
ns
*
*
Caudal
Medial
Rostral
B1
B2
B3
Hoescht / PCNA
% surface PCNA
ns
ns
**
Caudal
Medial
Rostral
C1
C2
C3
Hoescht / Iba1
Iba1+ cells counts (/mm² OM)
ns
*
*
Caudal
Medial
Rostral
20µm

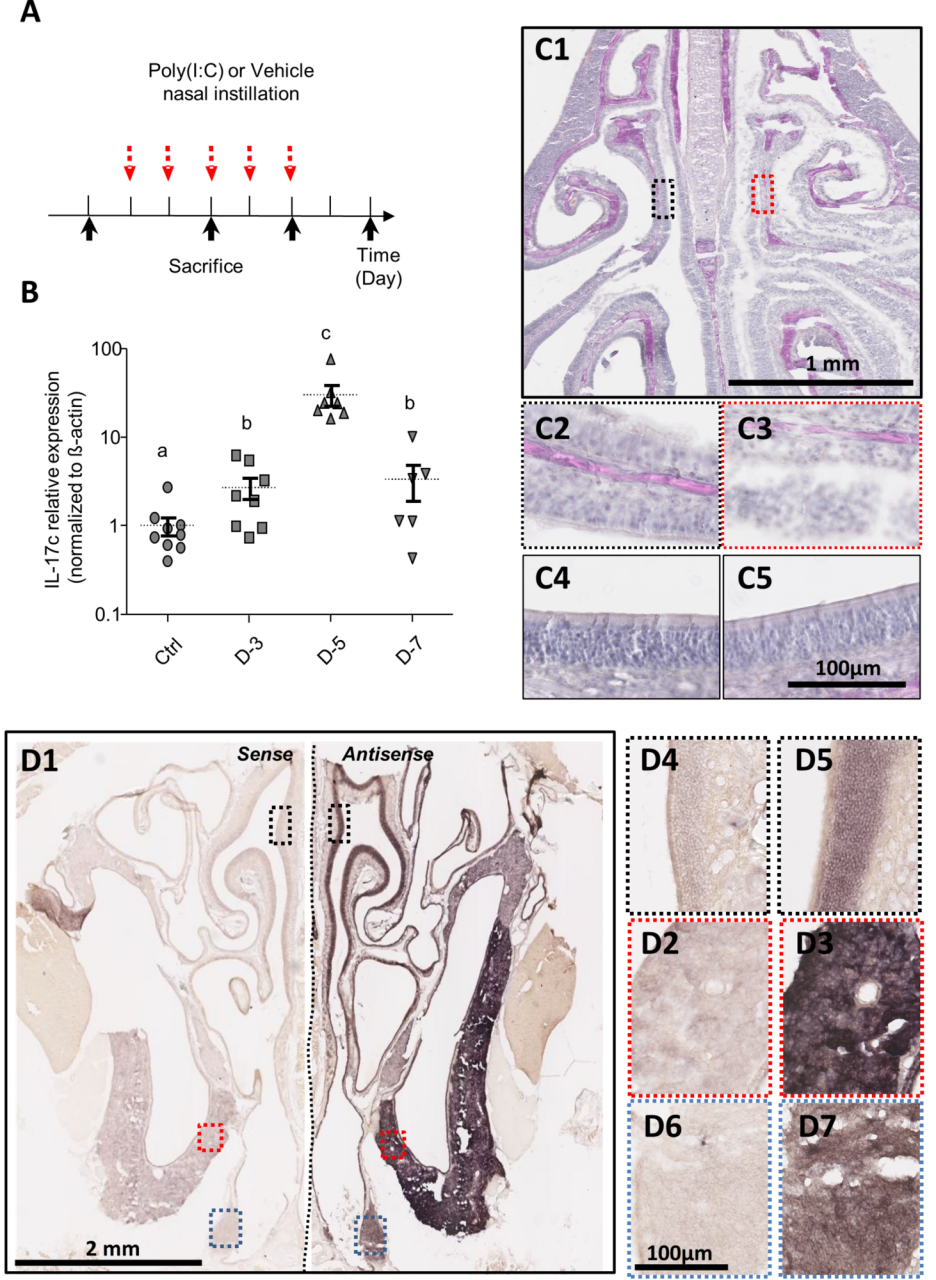
A
Poly(I:C) or Vehicle
nasal instillation
Sacrifice
Time
(Day)
B
IL-17c relative expression
(normalized to ß-actin)
100
10
1
0.1
a
b
c
b
Ctrl
D-3
D-5
D-7
C1
1 mm
C2
C3
C4
C5
100µm
D1
Sense
Antisense
2 mm
D4
D5
D2
D3
D6
D7
100µm

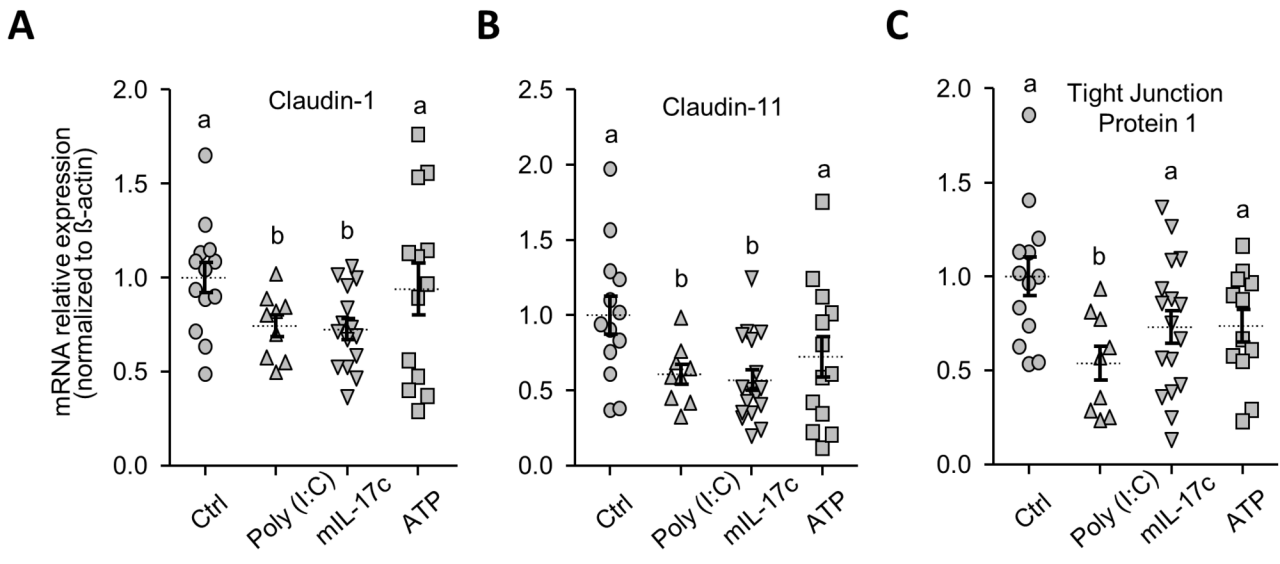
A
B
C
Claudin-1
Claudin-11
Tight Junction Protein 1
mRNA relative expression (normalized to ß-actin)
2.0
1.5
1.0
0.5
0.0
2.5
a
b
Ctrl
Poly (I:C)
mIL-17c
ATP

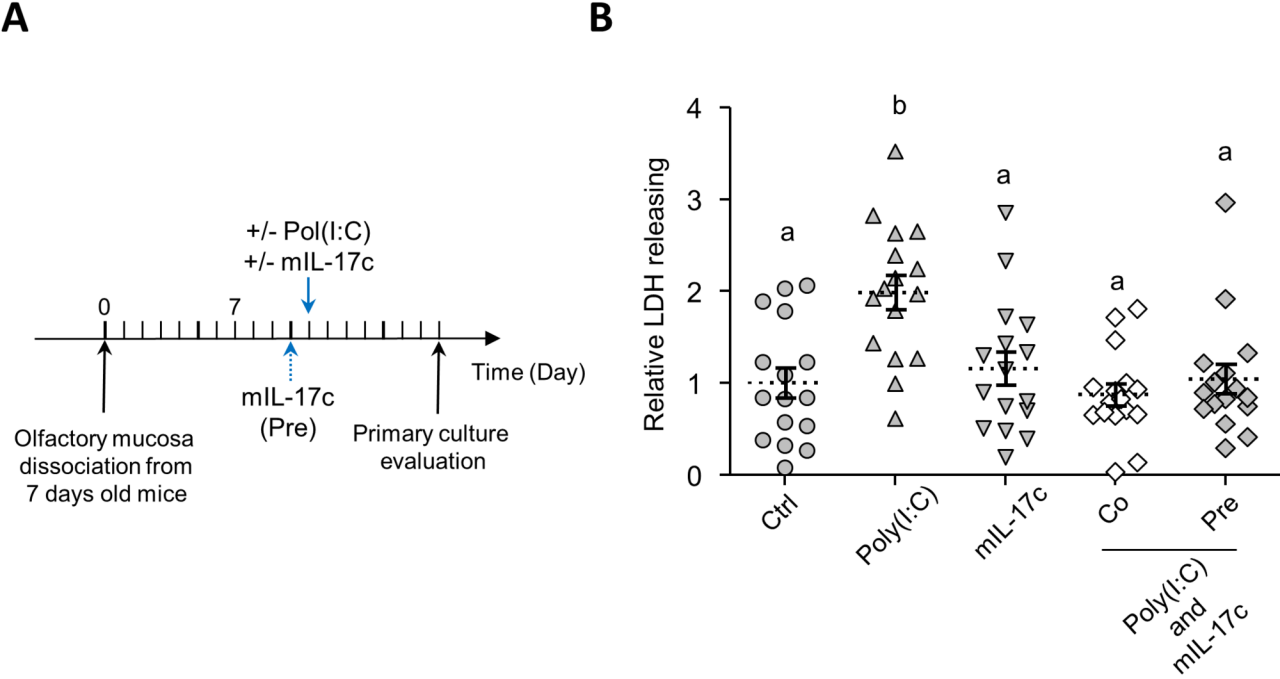
A
+/- Pol(I:C)
+/- mIL-17c
0
7
Time (Day)
mIL-17c
(Pre)
Olfactory mucosa
dissociation from
7 days old mice
Primary culture
evaluation
B
Relative LDH releasing
4
3
2
1
0
a
b
a
a
a
Ctrl
Poly(I:C)
mIL-17c
Co
Pre
Poly(I:C)
and
mIL-17c